D'Apuzzo 1 MPMI

1 **PII overexpression in *Lotus japonicus* affects nodule activity in permissive low**

2 **nitrogen conditions and increases nodule numbers in high nitrogen treated plants**

3 **Enrica D'Apuzzo[1;3], Vladimir Totev Valkov[1;3], Aurora Parlati[1], Selim Omrane[1], Ani**

4 **Barbulova[1], Maria Martha Sainz[1], Marco Lentini[2], Sergio Esposito[2], Alessandra**

5 **Rogato[1], Maurizio Chiurazzi[1]**

6 **[1] Institute of Biosciences and Bioresources, CNR, Via P. Castellino 111, Napoli, Italy**

7 **[2] Università degli Studi di Napoli Federico II, Dipartimento di Biologia, Via Cinthia**

8 **6, 80126, Napoli, Italy**

9 **[3] These authors contributed equally to this work**

10

11

12

13

14

15

16

17

18

19

20

21 **Present address: Ani Barbulova, Arterra Bioscience Srl, Via B. Brin 69, 80142,**

22 **Napoli, Italy; Maria Martha Sainz, Departamento de Nutrition Vegetal, Estacion**

23 **Experimental de Aula Dei, Consejo Superior de Investigationes Cientificas, 50080,**

24 **Zaragoza, Spain**

D'Apuzzo 2 MPMI

1 **Corresponding author**

2 **Dr. M. Chiurazzi: Tel. 0039-081-6132433; Fax: 0039-081-6132706; email:**

3 **maurizio.chiurazzi@ibbr.cnr.it**

4 **Abstract**

5 **We report here the first characterization of a *GLNB1* gene coding for the PII**

6 **protein in leguminous plants. The main purpose of this work was the investigation**

7 **of the possible roles played by this multi-functional protein in nodulation pathways.**

8 **The *Lotus japonicus LjGLB1* gene shows a significant transcriptional regulation**

9 **during the light-dark cycle and different nitrogen availability, conditions that**

10 **strongly affect nodule formation, development and functioning. We also report**

11 **analysis of the spatial profile of expression of Lj*GLB1* in root and nodule tissues and**

12 **of the protein's sub-cellular localization. Transgenic *Lotus japonicus* lines**

13 **overexpressing the PII protein were obtained and tested for the analysis of the**

14 **symbiotic responses in different conditions. The un-coupling of PII from its native**

15 **regulation affects nitrogenase activity and nodule polyamine content. Furthermore,**

16 **our results suggest the involvement of PII in the signaling of the nitrogen nutritional**

17 **status affecting the legumes predisposition for nodule formation.**

18

21

22

23

2

D'Apuzzo 3 MPMI

1 **Introduction**

2 The superfamily of PII signal transduction proteins represents one of the most widely

3 distributed signaling proteins in nature (Forchhammer 2004; Huergo et al. 2013). Many

4 bacteria and archaea have multiple PII proteins, whereas a single copy is found in plants

5 and most cyanobacteria. PII proteins are homotrimers composed of 12- to 13-kDa

6 subunits, forming a compact cylinder from which three long loops (the T loops) protrude

7 (Cheah et al. 1994; Vasudevan et al. 1994). The PII regulatory action in bacteria takes

8 place through a protein-protein interaction mechanism controlling the activities of a wide

9 range of targets, including enzymes, transcription factors and membrane transporters

10 mostly involved in nitrogen metabolism. Thereafter PII was also identified as a key C and

11 N metabolic integrator in early studies examining GS regulation (Moorhead and Smith

12 2003) and more recently, a biochemical characterization of bacterial PII proteins revealed

13 allosteric complexes involving ATP or ADP and 2-OG which function to sense cellular

14 energy and carbon levels (Jiang and Ninfa 2007). Layered on top of allosteric sensing of

15 cellular carbon and energy availability is the covalent modification of PII in response to

16 cellular nitrogen status. An ATPase activity has been formally proven in the PII paralog

17 GlnK leading to a model where the role of ATP/ADP binding is to effect a 2-OG-

18 dependent molecular switch that drives a conformational change in the T loop

19 (Radchenko et al. 2013). The convergence of these two types of input alters the ability of

20 PII to interact with partner proteins which in turn controls the ability of these partners to

21 modify various aspects of N metabolism, including gene transcription, membrane

22 transporters and metabolic enzymes (Moorhead and Smith 2003; Forchhammer 2008).

23 Carbon and Nitrogen requirements of plant cells can vary between tissue types, requiring

D'Apuzzo 4 MPMI

1   precise inter-tissue, and therefore, cellular cooperation. N taken up by roots mainly in the

2   form of nitrate and ammonium can be either used in root N metabolism or transported to

3   photosynthetic tissues for incorporation into amino acids. Conversely, carbon can be

4   fixed locally by photosynthetic processes and synthesized into the necessary C substrates

5   to supplement chloroplast-mediated nitrogen assimilation and amino acid biosynthesis, or

6   translocated in the form of sucrose from photosynthetic tissues to provide energy and

7   carbon skeletons for nitrogen assimilation in root tissues. In the case of leguminous

8   plants, nitrogen-fixing root nodules are the organs where atmospheric N reduction and

9   release take place and at the same time, optional C sink organs that need to assimilate

10   energy source either for the formation of nodule primordium (Complainville et al. 2003),

11   and to provide energy for the N fixation performed by the microsymbiont (*Rhizobium*)

12   and assimilation of the produced ammonium and starch biosynthesis (Vance 2008).

13   Despite the central role played as an integrator of C and N cellular metabolism in many

14   prokaryotes, plant PII is a nuclear-encoded chloroplast protein (GLB1) that seems to have

15   evolved secondary, tissue-specialized roles. Preliminary studies suggested a conserved

16   role as nitrogen/carbon sensor due to the lack of glutamine sensing in *A. thaliana* PII

17   overexpressors (Hsieh et al. 1998). Later, PII has been implicated in the control of the

18   arginine (Arg) biosynthetic pathway, through interaction with NAGK (Burillo et al. 2004;

19   Sugiyama et al. 2004; Ferrario-Mery et al. 2006) to reduce feedback inhibition by high

20   Arg concentrations (Maheswaran et al. 2004; Ferrario-Mery et al. 2006; Chen et al.

21   2006). The plant complex PII-NAGK only shows gradual inhibition of complex

22   formation at 2-OG concentrations greater than 1 mM (Mizuno et al. 2007a; Beez et al.

23   2009). Most recently major fluctuation of the *GLB1* transcript during seed maturation in

4

D'Apuzzo 5 MPMI

1   *A. thaliana* (Uhrig et al. 2009) was associated to a crucial role played by PII in the fine

2   tuning of fatty acid biosynthesis and partitioning in Arabidopsis seeds (Baud et al. 2010).

3   In addition, two PII target proteins in *A. thaliana* that are biotin carboxyl carrier subunits

4   of the plastidial acetyl-CoA-carboxylase (ACCase), namely BCCP1 and BCCP2,

5   involved in the production of the precursor of lipid biosynthesis, malonyl-CoA have been

6   identified (Feria Bourellier et al. 2010). ACCase activity was inhibited by PII in

7   chloroplast extracts, in the presence of MgATP, while the addition of 2-OG, pyruvate or

8   oxalacetate was sufficient to release the inhibition, thus suggesting for the first time the

9   involvement of PII in the regulation of an enzyme dedicated to carbon metabolism (Feria

10 Bourellier et al. 2010).

11 We report here the first characterization of the *GLB1* gene in a leguminous plant with a

12 detailed analysis of the transcriptional regulation in different growth conditions

13 metabolically linked to the symbiotic nitrogen fixation process. Phenotypic analysis of

14 transgenic *L. japonicus* overexpressing lines revealed a putative novel role of PII in the

15 control of nodule functioning phenotypes and involvement in the signaling pathways

16 governing N-dependent nodulation competence.

17

18 **Results**

19 ***Identification of the L. japonicus sequence encoding for the PII protein and***

20 ***description of its structural features***

21 Blast search for orthologs of the *Medicago Sativa* PII protein (Accession number

22 AY027892) in the *L. japonicus* genome sequence database

23 (http://www.kazusa.or.jp/lotus) identified a single copy gene (chr1.CM0122.1600.r2.m)

D'Apuzzo 6 MPMI

1   coding for a 195 amino acid protein with a molecular mass of 21.49 kDa sharing 70% aa

2   identity with the *M. sativa* PII protein. The genomic locus consists of eight exons

3   separated by seven introns (Supplementary Fig. S1) with a gene structure identical to that

4   identified in *A. thaliana* (AT4G01900). Multiple sequence alignment recognized the

5   region (pos. 106-124) highly conserved between bacteria and plant PII proteins (the T-

6   loop motif) that plays a key role in mediating interactions between PII and downstream-

7   effector proteins (Mizuno et al. 2007b; Sant'anna et al. 2009). In particular, amino acids

8   residues involved in the 2-OG-dependent conformational change of the T-loop

9   (Radchenko et al. 2013) are conserved in the *L. japonicus* sequence (Q108 and K128).

10   Furthermore, highly conserved charged amino acids likely to be involved in homotrimer

11   formation in *A. thaliana* are identical in the *L. japonicus* sequence corresponding to K72,

12   E74, D101, R103, K130 and E132 (Smith et al. 2003). The N- and C-terminal plant PII

13   signatures are also identified in the Lotus sequence (pos. 69-81 and 173-188,

14   respectively). The molecular phylogenetic tree (Fig. 1) based on the alignment of

15   complete amino acid PII sequences and drawn using the Neighbor-Joining method

16   (Saitou and Nei 1987) integrates the taxonomic analysis previously reported (Uhrig et al.

17   2009), indicating a close relationship among the PII legume sequences.

18

19   ***Transcriptional regulation of LjGLB1 in response to light-dark cycle and N supply***

20   In the literature most of the reported transcriptional analyses of *GLB1* gene use leaf

21   tissues to investigate a possible mechanism of control associated with dark/light cycle

22   and/or C supply derived from photosynthesis. Our analysis of *LjGLB1* was especially

23   aimed to investigate a possible regulation of the transcriptional profile in both

D'Apuzzo 7 MPMI

1 photosynthetic (leaves) and non photosynthetic organs (roots and nodules) under

2 conditions that may affect symbiotic performances. We first analysed by qRT-PCR the

3 distribution of the *LjGLB1* transcript in different organs of *L. japonicus*. The amount of

4 *LjGLB1* transcript didn't change significantly between root and leaf tissues of plants

5 grown on Gamborg-B5 derived media with 1 mM ammonium nitrate as N source or

6 without N (Fig. 2A). In the latter conditions plants were inoculated with *M. loti* to test

7 *GLB1* expression in mature nodules and a comparable level of transcript was detected in

8 nodular tissue suggesting that PII might be performing some roles in this organ (Fig. 2A).

9 The *GLB1* transcriptional analysis during the dark/light cycle (8hr/16hr) in hydroponic

10 cultures of *L. japonicus* plants is reported in Fig. 2 B and 2C. A rapid enhancement

11 (about four fold) of *GLB1* transcription in roots was revealed at 3 hours from the

12 beginning of the light cycle with the amount of transcript remaining constant till the end

13 of the light period and starting to decay after two hours until the end of the dark period

14 (Fig. 2B). A similar trend of transcriptional regulation was detected in leaves under the

15 same experimental conditions (Fig. 2C). In both root and leaf tissues the presence of 3%

16 sucrose in the growth medium doesn't affect the level of expression during the light

17 period. However, the effect of light on *GLB1* mRNA could be mimicked, both in root and

18 leaf tissues, at the end of the dark period, by the addition of 3% sucrose indicating that in

19 *L. japonicus* the effect of light on *GLB1* transcription is mediated by photosynthetic

20 products (Fig. 2B and C).

21 *GLB1* transcription was further examined in roots of *L. japonicus* plants grown in

22 hydroponic cultures for two weeks in N-sufficient conditions (1mM ammonium nitrate)

23 and then transferred to fresh nutrient solution containing no nitrogen source. To minimize

D'Apuzzo 8 MPMI

1   the diurnal changes in the expression level, all samples were taken in the middle of the

2   light time (6 hr in Fig. 2) and RNA was extracted from roots at time 0, 24 hrs, 48 hrs, 72

3   hrs and 5 days after the shift. The *LjGLB1* transcription showed a rapid down-regulation

4   (4 fold) that was maintained until at least 72 hrs after the shift (Fig. 3). Interestingly, the

5   amount of *LjGLB1* transcript in roots increased again after 5 days on N-starvation

6   condition, to the basal level observed at T0 (Fig. 3). As a control of the experimental

7   conditions we analyzed the expression profile of the high affinity ammonium transporter

8   *LjAMT1;1* that, as expected, was strongly induced after the shift from N-sufficient to N-

9   starvation conditions (Fig. 3; D'Apuzzo et al. 2004). Therefore, our results indicated a

10   significant regulation of the *GLB1* expression at the transcriptional level that takes place

11   either in leaves and root tissues.

12

13   ***PII localization and spatial profile of expression***

14   Unlike other plant PII proteins, the Lotus sequence didn't show a clear-cut N-terminal

15   transit peptide for chloroplast targeting according to the prediction program CHLOROP

16   (**http://www.cbs.dtu.dk/services/ChloroP**). Therefore, in order to check the PII protein

17   sub-cellular localization, we fused its C-terminal end without a stop codon, to the *GREEN*

18   *FLUORESCENT PROTEIN* (*GFP*) gene, and placed the fusion downstream of the

19   CAMV-35S promoter. Confocal laser-scanning fluorescence microscopy in stable

20   transgenic hairy roots indicated unambiguously a plastid localization of GFP in roots,

21   confirming previous data obtained in Arabidopsis and rice (Hsieh et al. 1998; Sugiyama

22   et al. 2004; Baud et al. 2010). The specificity of the plastids as target was indicated by

D'Apuzzo 9 MPMI

1   co-localization with the red fluorescence of the *AtrecA*-DsRed2 fusion (Supplementary

2   Fig. S2 A-C; Kohler et al. 1997).

3   To gain further information about the profile of *LjGLB1* expression in roots and nodules,

4   we isolated the 5' region of the gene to obtain a T-DNA construct carrying a promoter-

5   *gus*A fusion. A PCR fragment extending up to 980 bp upstream of the ATG of *LjGLB1*

6   and including the first 21 PII codons was subcloned in the pBI101.1 binary vector to

7   obtain a translational fusion with the *gus*A reporter gene (Jefferson 1987). *Lotus*

8   composite plants obtained upon transformation with *Agrobacterium rhizogenes*

9   (Martirani *et al.* 1999) were used to analyse the expression of the translational p*LjGLB1*-

10   *gus*A fusions in a hairy root system. In the root tissues GUS activity was substantially

11   limited to the stele where it was detected in 100% of the stained roots (Fig. 4A). In some

12   cases a longer incubation time allowed the detection of the blue staining in cortical cells

13   and cap cells, while no activity could be observed in meristematic regions (Fig. 4B, C).

14   Root cross sections allowed the definition of a more precise pattern showing a

15   distribution of GUS activity inside the endodermis cell layer with the main staining

16   apparently located in the primary phloematic space (Fig. 4D). The promoter activity of

17   the *A. thaliana GLB1* gene has been described in leaf vascular structures only in an over-

18   expressing Arabidopsis WRl1 genotype (Baud et al. 2009 and 2010). However, analysis

19   of the 980 bp 5' UTR *LjGLB1* region exploited for driving the *gus*A expression in

20   transgenic hairy roots didn't reveal any of the 15 bp boxes (cAAAAGtAggggttT)

21   reminiscent of the consensus sequence required for WRl1 induction of glycolitic and fatty

22   acid biosynthetic genes (Baud et al. 2010), while only one putative AW-box motif

23   (CnTnGn$_7$CG; Maeo et al. 2009) was found at position -231 relative to the translational

D'Apuzzo 10 MPMI

1   start codon (data not shown).

2   The profile of *LjGLB1* promoter activity was also analyzed during different steps of

3   nodule development and/or function. GUS activity was never induced during the initial

4   stages of *M. loti* infection whereas the analysis in young and mature nodules allowed the

5   detection of a strong blue staining in the nodule vascular bundles, with a weaker activity

6   in the nodule parenchyma (Fig. 4E). The absence of *LjGLB1* transcriptional regulation

7   early after inoculation was also confirmed by the qRT-PCR analysis shown in

8   Supplementary Fig. S3. In addition, the observed N-dependent transcriptional regulation

9   together with the reported impact of the photosynthate supply on the *LjGLB1*

10 transcriptional profile (Fig. 2 and 3) prompted us to investigate the relationship between

11 nodular *LjGLB1* expression and nitrogen fixation activity. Therefore, the pattern of GUS

12 activity was evaluated in young nodules obtained with a *M. loti fix⁻* mutant. The

13 transgenic nodules obtained in hairy roots inoculated with either wild type or a *nifH*

14 mutant didn't show any change in the quantitative and qualitative GUS activity

15 distribution (data not shown).

16

17 ***Generation of transgenic L. japonicus plants ectopically expressing the GLB1 gene***

18 In order to test whether the *GLB1* gene in legumes plays any role in the formation and/or

19 functioning of nitrogen-fixing-nodules, a process strictly dependent by a correct C/N

20 balance, we cloned the *LjGLB1* coding sequence between a CaMV-35S promoter

21 sequence and a tNOS terminator sequence (Hajdukiewicz et al., 1994) to obtain

22 transgenic PII over-expressing Lotus plants. Primary transformed plants were selected on

23 hygromicin medium and allowed to self-pollinate. Independent T1 lines, germinated on

D'Apuzzo 11 MPMI

1   hygromicin (Hygromycin Resistance segregation 3:1), were tested by semiquantitative

2   RT-PCR to analyze the level of *GLB1* transcript and transgenic lines with various level of

3   over-expression were identified. T2 homozygous plants 7-13 and 8-9, showing 5 and 10

4   fold increase of the *LjGLB1* transcript were selected for further phenotypic analysis (Fig.

5   5A). To verify proper protein synthesis of the ectopically expressed gene, Western blot

6   analysis was performed on crude protein extracts from the transgenic and wild type plants

7   and PII was detected using a polyclonal antiserum raised against recombinant *A. thaliana*

8   PII protein (Ferrario-Mery et al. 2005). Fig. 5B shows a linear increase of the PII protein

9   in the transformants, proportional to the observed induced amount of transcript when

10   compared to the wild type plant.

11

12   ***Phenotypic characterization of PII overexpressing plants***

13   The spatial profile of *GLB1* promoter activity in the nodular tissue prompted us to test

14   whether the PII protein could play a role as an integrator of the carbon, nitrogen and

15   energy levels that are critical for a correct nodule organogenesis and functioning. A

16   comparison of the nodulation response in Lotus wild type and PII over-expressing

17   seedlings grown on low N supply (10 μM NH_4NO_3) and inoculated with *M. loti*,

18   indicated equivalent phenotypes in terms of nodule numbers (Fig. 6A), nodule mass (data

19   not shown) and structural organization (Supplementary Fig. S4A). On the other hand,

20   analysis of N fixation activity at 28 days after inoculation indicated a significant 30%

21   reduction in nodules of PII-overexpressing plants (Fig. 6B). However, this deficiency was

22   not sufficient to cause a significant difference in terms of fresh shoot weight that was

23   comparable in the two plant genotypes (Supplementary Fig. S4B). Since, Ferrario-Mery

11

D'Apuzzo 12 MPMI

1   et al. (2006) reported a reduction of several products of the ornithine/arginine biosyntetic

2   pathway in *A. thaliana* PII knock-out mutants in response to ammonium resupply after N

3   starvation, we tested the content of polyamines, which are the final products of this

4   biosynthetic pathway and have been involved in the regulation of symbiotic efficiency,

5   in PII overexpressing plants. Polyamines were extracted in mature nodules of plants

6   grown in 10 μM NH_4NO_3 and their relative amounts compared in wild type and 8-9

7   plants. The content of spermidine and spermine were much higher than that of citrulline

8   and didn't change significantly between wild type and overexpressing plants, whereas the

9   citrulline level was strongly increased (6.5 fold) in nodules of the 8-9 plants (Fig. 6C and

10 D).

11 N depletion in the soil is a prerequisite for nodule development and function, and high

12 concentrations of nitrogen as nitrate and ammonia might abolish nodulation. We reported

13 a link between the *L. japonicus* N nutritional status and nodule capacity predisposition

14 showing that the competence for nodulation of *L. japonicus* plants pre-incubated, prior to

15 the *M. loti* inoculation, on high N (10 mM NH_4NO_3) conditions was significantly reduced

16 (about 50%) when compared to plants maintained in low N (10 μM NH_4NO_3) permissive

17 conditions (Omrane et al. 2009). The inhibitory effect was maintained for at least six days

18 in Lotus plants pre-incubated on high N, indicating that it was correlated to a systemic

19 change of the general N nutritional state of the plants that was transduced to the root

20 nodulation machinery (Omrane et al. 2009). Therefore, in order to analyze any possible

21 involvement of the PII protein in the signal transduction route connecting N nutritional

22 status and nodulation capacity we compared the nodule formation phenotype of wild type

23 and PII over-expressing plants following the experimental scheme reported in Omrane et

D'Apuzzo 13 MPMI

1   al. (2009). As shown in Fig. 7A, wild type *L. japonicus* plants pre-incubated on 10 mM

2   ammonium nitrate showed a reduced number of nodules when compared to plants

3   maintained on 10 μM ammonium nitrate (Fig. 7A; 3.37 vs 1.75 nodules per plant).

4   Strikingly, both over-expressing 7-13 and 8-9 PII lines were able to rescue this inhibitory

5   effect, showing the same level of nodulation capacity in low and high N conditions (Fig.

6   7A). In *L. japonicus* a central role of the CLE glycopeptide *Lj*CLERS2 in the nitrate-

7   induced systemic suppression of nodulation through interaction with HAR1 receptor

8   kinase has been reported (Okamoto et al 2009; Okamoto et al. 2013). In order to test

9   whether PII overexpression could induce a de-regulation of *LjCLERS2* we compared the

10   amount of transcript in wild type and PII overexpressing plants incubated for 10 days in

11   low and high NH_4NO_3 conditions. Consistently with data reported in the literature

12   *LjCLERS2* was induced in Lotus wild type plants incubated on higher N concentrations

13   when compared to plants grown on 10 μM NH_4NO_3 permissive conditions and a similar

14   pattern was observed in the 8-9 plants (Fig. 7B).

15

16   **Discussion**

17   How PII is regulated in higher plants and hence how this transduction protein can sense

18   the C/N status of a plant is still a matter of debate. A post-translational control of its

19   activity similar to that of PII from prokaryotes has not been demonstrated yet (Smith et

20   al. 2004). In oxygenic photosynthetic organisms the PII interaction with NAGK, the key

21   enzyme of the arginine bio-synthesis pathway, enhances the catalytic kinase activity and

22   leads to the relieve of the feedback inhibitory effect by the final pathway product,

23   arginine (Chen et al. 2006; Ferrario-Mery et al. 2006). PII in the ATP-ligated state has a

D'Apuzzo 14 MPMI

1   very high affinity for NAGK, whereas ADP and 2-OG display a non antagonizing

2   inhibitory effect on the formation of the PII-NAGK complex, which therefore seems not

3   governed by the intrinsic ATPase activity of PII (Maheswaran et al. 2004; Zeth al. 2014).

4   2-OG has been also proposed as the main signal controlling the PII inhibition of ACCase

5   in chloroplast extracts, thereby expanding plant PII function beyond N regulation (Feria

6   Bourellier et al. 2010).

7   With regard to the role played by a transcriptional regulation on the *GLB1* gene, recently

8   a striking observation reporting the up-regulation of the PII transcript (10 fold) in the

9   early- to mid-stages of *A. thaliana* developing seeds strongly supported an involvement

10   of such a mechanism of regulation in the control of plant PII function (Uhrig et al. 2009).

11   Partially inconsistent data were reported for the transcriptional level of regulation of the

12   *GLB1* gene expression in leaves (Hsieh et al. 1998, Ferrario-Mèry et al. 2005). A strong

13   and rapid activation of *GLB1* transcription was first reported in dark-adapted Arabidopsis

14   plants after a shift in light conditions and this derived, at least in part, from

15   photosynthetic products (Hsieh et al. 1998). On the other hand, a stable amount of the

16   *GLB1* transcript was observed in Arabidopsis rosette leaves during most of the day/night

17   cycle with a slight increase only at the end of the day (Ferrario-Mèry et al. 2005). We

18   analyzed the profile of *LjGLB1* expression in both Lotus root and leaf tissues and found a

19   rapid induction of the *LjGLB1* transcript during the light period. This effect could be

20   mimicked, during the dark period, by the addition of 3% sucrose, indicating that

21   induction of the transcription is mediated by the sensing of photosynthetic products (Fig.

22   2). We also observed a N-dependent regulation of transcription with a rapid and transient

23   decrease of the amount of *LjGLB1* transcript followed by a progressive increase in roots

D'Apuzzo 15 MPMI

1   of plants transferred into N-starvation conditions (Fig. 3). This latter result might be

2   consistent with data reported in *A. thaliana,* where the *AtGLB1* transcript level, was

3   analyzed only 5 days after a shift to N-deficiency condition and showed no significant

4   variation (Ferrario-Mèry et al. 2005). Thus, our results indicate that a significant part of

5   the regulation of the *LjGLB1* profile of expression takes place at the transcriptional level.

6   The growth conditions tested in this work (different N and C sources availability)

7   significantly affecting the regulation of *LjGLB1* gene expression (Fig. 2 and 3) might

8   strongly impact the efficiency of symbiotic-nitrogen-fixation process (nodule formation,

9   developing and functioning). Photosynthate resources must be allocated to the nodules

10   where carbon derived from the metabolism of sucrose, is used for several physiological

11   processes, including plant and bacterial respiration, assimilation of fixed N_2 and starch

12   and cellulose biosynthesis (Tsikou et al. 2013). Furthermore, a strict interdependence

13   exists between the level of nitrogenase activity and the efficiency of carbon sources flux

14   providing energy for the bacteroid-mediated N_2 reduction (Pathirana et al. 1992; Schulze

15   et al. 1998). On the other hand, limitation of combined N in the soil is a prerequisite for

16   initiation, development and functioning of N-fixing nodules (Bisseling *et al.* 1978;

17   Caetano-Anollès and Gresshoff 1991; Matamoros et al. 1999; Barbulova *et al.* 2007) and

18   legumes employ a number of regulatory mechanisms to avoid nodulation under N-replete

19   conditions, when sufficient mineral or organic nitrogen is available in the soil, restricting

20   nodulation to sustainable levels only when soil nitrogen is limiting (Omrane and

21   Chiurazzi 2009).

22   As preliminary tool to initiate studies on the putative role played by the PII protein during

23   the nodulation process we exploited two transgenic overexpressing lines in which

15

D'Apuzzo 16 MPMI

1   *LjGLB1* expression is un-coupled from its native regulation (Fig. 5). PII overexpressing

2   plants grown on low N permissive conditions, do not show differences in terms of nodule

3   formation capacity, whereas a significant 30% reduction of Nitrogenase Activity

4   measured as Acetylene Reduction Activity (ARA) was observed when comparised to

5   wild type plants (Fig. 6A, B). However, in the exploited experimental system where 10

6   μM KNO_3 is present as N source this nodular activity defect is not sufficient to affect

7   normal shoot growth phenotype (Supplementary Fig. S4B).

8   The spatial profile of the *LjGLB1* promoter activity shown in Fig. 4, which to our

9   knowledge represents the first information reported in the literature about the PII

10   distribution in root tissues, indicates a main localization in vascular bundles (Fig. 4). Root

11   vascular structures mediate long-distance transport of compounds such as N metabolites

12   and sucrose from root to shoot and vice versa. Hence this spatial profile of PII

13   localization might be consistent with both transcriptional patterns shown in Fig. 2 and 3

14   where regulation of the *LjGLB1* expression was reported to be controlled by

15   photosynthetic products and N supply conditions.

16   However, the expression pattern of *LjGLB1* promoter activity in nodule vascular bundles

17   and parenchima (Fig. 4E) might provide an additional clue about a possible link between

18   PII function and the observed ARA defective phenotype, as this partially overlaps the

19   ones of *L. japonicus* genes encoding spermidine synthase, spermine synthases, arginine

20   decarboxylase and ornithine decarboxylase (*LjSPDS*, *LjSPMS, LjADC, LjODC*), involved

21   in the synthesis of polyamines spermidine and spermine from putrescine and mainly

22   expressed in the nodule parenchima and vascular bundles (Flemetakis et al. 2004; Efrose

23   et al. 2008). A high content of putrescine, spermine and spermidine in mature nodules,

D'Apuzzo 17 MPMI

1   with an increased amount compared to other legume organs has been already reported

2   (Fujihara et al. 1994; Flemetakis et al. 2004). The *LjODC* gene encodes ornithine

3   decarboxylase which catalyzes the synthesis of ornithine to putrescine, the obligate

4   precursor of spermidine and spermine (Fig. 8) and a root/nodule specific expression

5   profile for *LjODC* has been detected, with a strong induction observed during nodule

6   development (Flemetakis et al. 2004). Our analysis of polyamine content in wild type

7   nodules with the lower level of citrulline compared to spermine or spermidine (Fig. 6C

8   and D) suggests the occurrence in nodular tissue of a metabolic shunt of ornithine into

9   putrescine for polyamine biosynthesis through the action of ODC, rather than the

10   alternative pathway catalyzed by ornithine transcarbamylase (OTC) that utilizes the same

11   substrate (ornithine) for the synthesis of citrulline (Fig. 8) and this hypothesis is

12   consistent with the previously reported *LjODC* profile of expression (Flemetakis et al.

13   2004). The high level of spermine and spermidine was not affected in nodules of PII

14   overexpressing plants (Fig. 6C) where we observe a clear-cut 10 fold increase of the

15   citrulline content when compared to wild type (Fig. 6D). The biosynthetic pathway

16   involving the enzymes ODC, ADC, SPDS, and SPMS is controlled by the major plant

17   PII-interacting protein, NAGK (Fig. 8; Burillo et al. 2004; Sugiyama et al. 2004;

18   Ferrario-Mery et al. 2006) and the increased level of citrulline observed in nodules of the

19   PII overexpressing plants (Fig. 6D) is consistent with the reduced ornithine, citrulline and

20   arginine accumulation observed in Arabidopsis PII knock-out mutants (Ferrario-Mery et

21   al. 2006). The reason we didn't observe a parallel increase of the spermine and

22   spermidine levels could be a consequence of the hypothesized metabolic shunt leading to

23   a high basal level of these polyamines in wild type nodules. Polyamines are important

1   components for the establishment of optimal symbiotic performance and a negative effect

2   of high concentration of exogenous putrescine on ARA activity has been reported

3   (Wisniewski and Brewin 2000). Therefore, the reduced nitrogen fixation activity

4   observed in PII overexpressing plants could be related to the increase of nodular

5   polyamines through the ornithin biosyntetic pathway.

6   The other clear-cut phenotype scored in the PII overexpressing lines is the capacity of

7   responding very effectively to a preliminary high N treatment, prior to *M. loti*

8   inoculation, that causes about a 50% reduction in the nodulation rate of wild type *L.*

9   *japonicus* plants, completely rescuing this deficient phenotype (Fig. 7A; Omrane et al.

10   2009). Therefore, our results suggest that the PII protein in legumes may serve as part of

11   a complex signal transduction network involved in perceiving the N status of the plant

12   and regulating nodulation capacity predisposition. In legumes a systemic adaptation

13   mediated by plant N status regulating nodule formation has been demonstrated (Jeudy et

14   al. 2010) and affymetrix geneChip analyses indicate a strong systemic influence of the N

15   supply on the profile of gene expression in roots before and after inoculation (Ruffel *et*

16   *al.* 2008; Omrane et al. 2009). The reported effect of PII overexpression on the

17   ornithine/arginine biosyntetic pathway (Fig. 6D) could be also correlated to the improved

18   nodulation response of Lotus plants to high N conditions (Fig. 7A) as polyamines might

19   also affect nodule formation capacity and in particular a positive effect of citrulline

20   supply on the formation of infection threads structures in *L. japonicus* nodules has been

21   reported (Mishima et al. 2008). Another intriguing correlation to the increased level of

22   citrulline could be a positive effect of PII overexpression on the arginine-dependent

23   synthesis of nitric oxide (NO; Fig. 8) that plays a direct role on the nodule formation

D'Apuzzo 19 MPMI

1   process as a depletion of this signal causes down-regulation of plant genes involved in

2   nodule development and formation (Del Giudice et al. 2011; Boscari et al. 2013), and a

3   significant decrease of nodule number (Pauly et al. 2011; Del Giudice et al. 2011).

4   However, our data indicate that one of the actor playing a crucial role in the nitrate-

5   dependent control of nodule initiation, *LjCLERS2* (Okamoto et al 2009; Okamoto et al.

6   2013) is likely not to be a target of the PII action, as its transcriptional profile did not

7   change in overexpressing plants (Fig. 7B). Nitrate may affect lateral root development

8   (Zhang et al. 1999) as well as nodule formation (Omrane and Chiurazzi 2009) by acting

9   both as a nutrient, through the assimilation pathways and consequent change of the

10   systemic general nutritional status or as a local signal independent of its assimilation.

11   *LjCLERS2* is a root specific gene and its nitrate dependent induction could be mediated

12   by a local signaling pathway followed by the systemic transmission through xylem of the

13   arabinosylated form of the peptide to the shoot where the interaction with the HAR1

14   (Hypernodulation Aberrant Root Formation) receptor kinase takes place, controlling the

15   process of nodule formation autoregulation (Okamoto et al. 2013). The *LjGLB1* gene is

16   ubiquitously expressed in Lotus plants (Fig. 2A) and PII protein likely acts by perceiving

17   the general N nutritional change determined by nitrate supply conditions. Therefore,

18   *Lj*CLERS2 and PII might be part of two different nitrate dependent regulatory pathways

19   controlling the nodule formation capacity and this would explain the conserved

20   *LjCLERS2* profile of expression observed in wild type and PII overexpressing plants (Fig.

21   7B).

22   In conclusion, our data suggest a possible novel role of the legumes PII protein in the

23   control of nodule functioning and signalling pathways linking N nutritional status and

D'Apuzzo 20 MPMI

1 nodulation competence. Ultimately, a global metabolomic analysis in the PII

2 overexpressing plants and the use of RNAi constructs driven by the *LjGLB1* own

3 promoter, vascular bundle-specific and/or nodule-specific promoters will allow us to gain

4 further insights into such functional roles of PII.

5

6 **Materials and Methods**

7 **Plant material and growth conditions**

8 All experiments were carried out with *Lotus japonicus* ecotype B-129 F12 GIFU.

9 Sterilized seeds were sown on H_2O agar plates and left over night at 4°C cap-side down.

10 After 24 hrs in the dark in the growth chamber, Petri dishes were exposed to light and

11 kept in a vertical position. Care was taken to maintain the young emerging roots in

12 contact with the filter paper. For the analysis of nodulation capacities, unsynchronized

13 seedlings were discarded at this stage. Plants were cultivated in a growth chamber with a

14 light intensity of 200 μmol m^{-2} sec^{-1} at 23°C with a 16 hr/8 hr day/night cycle. Solid

15 growth substrate had the composition of B5 medium (Gamborg 1970), except that, when

16 needed, $(NH_4)_2SO_4$ and KNO_3 were omitted and/or replaced by ammonium nitrate

17 (NH_4NO_3). KCl was added to the medium to replace the potassium source. The media

18 containing vitamins (Duchefa catalogue G0415) were buffered with 2.5 mM 2-(N-

19 Morpholino)-Ethanesulfonic Acid (MES; Duchefa, MIS03.0250) and pH was adjusted to

20 5.7 with KOH.

21 Experimental conditions for the analysis of the high N pre-incubation effect on

22 nodulation have been described in Omrane et al. (2009). 3-5 days old seedlings were

23 transferred and grown for ten days on B5 derived medium where $(NH_4)_2SO_4$ and KNO_3

D'Apuzzo 21 MPMI

1   were omitted and replaced by 10 mM (High-N) or 10 μM (Low-N) NH_4NO_3. KCl was

2   added to the medium to replace the potassium source. During these ten days

3   preincubation, plants were transferred twice on fresh media to avoid nutrient depletion.

4   After ten days, both High-N and Low-N plants were transferred onto fresh 10 μM

5   NH_4NO_3 medium and inoculated with *M. loti*. Six days after inoculation, plants were

6   transferred onto 10 μM NH_4NO_3 medium with addition of cefotaxime at 50 mg/L^{-1}.

7   Hydroponic colture conditions for the analysis of N- and light/dark cycle-dependent

8   *LjGLB1* regulation have been described in D'Apuzzo et al. (2004). One week old plants

9   germinated on solid medium were transferred into vessels harbouring 8 plants in about

10   100 ml of the 1mM NH_4NO_3 B5 derivative medium. In the Nitrogen-free solution the

11   NH_4NO_3 was omitted. The pH of the media were adjusted to 5.7 with MES. To avoid

12   depletion, the nutrient solution was renewed every three days during the ten days of

13   growth in hydroponic cultures. The pH of the medium was checked daily and it was

14   maintained within close limits (5.8 – 5.6) in all the conditions of hydroponic growth.

15   Plants were cultivated in a growth chamber with a light intensity of 200 μmol m^{-2} sec^{-1} at

16   23°C with a 16 hr/ 8 hr day/night cycle.

17   The *Mesorhizobium loti* strain R7A was used for the inoculation experiments and was

18   grown in liquid TY-medium supplemented with rifampicin (20 mg/L). The *M. loti nifH*

19   strain was kindly provided by Dr. Clive Ronson (University of Otago, New Zealand) and

20   was grown in the same medium supplemented with rifampicin and gentamicin (10 mg/L).

21   The inoculation procedure (10^7 cells per root tip) for the *in vitro* nodulation assay have

22   been reported elsewhere (Barbulova *et al.* 2005).

D'Apuzzo 22 MPMI

1   *L. japonicus* **transformation procedures**

2   *Agrobacterium rhizogenes*-mediated *L. japonicus* transformations were performed as

3   described in Martirani et al. (1999).

4   **T-DNA constructs preparation**

5   To obtain the PII over-expressing construct the *LjGLB1* cDNA was amplified with the

6   two oligonucleotides 5'- GAAGATCTATGGCGATTGCGAGAACGCAC-3' (including

7   a *Bgl*II site) and 5'- ACGCGTCGACTCATACAGTAGATAATATGTC-3' (including a

8   *Sal*I site) and subcloned as *Bgl*II-*Sal*I fragment into pCAMBIA1300 *BglII-Sal*I double

9   digested.

10   The 35S-*GLB1-GFP* fusion was prepared in the following way: the *LjGLB1* cDNA

11   sequence   was   amplified   with   the   two   oligonucleotides   5'-

12   GAGGATCCATGGCGATTGCGAGAACGCAC-3' (including a *Bam*HI site) and 5'-

13   GCGGTACCTACAGTAGATAATATGTCAGT-3' (including a *Kpn*I site), cloned into

14   the double-digested *Bam*HI-*Kpn*I β-GFP plasmid (Duby et al., 2001) and the correct

15   sequence for the *Lj*GLB1-GFP translational fusion was verified by sequencing. The

16   *LjGLB1-GFP* cassette was then cloned as a *Bam*HI-*Sac*I fragment into the double

17   digested *Bgl*II-*Sac*I pCAMBIA1300 vector.

18   The pLjGLB1-*gus*A fusion was prepared in the following way: a PCR amplified

19   fragment was obtained on genomic DNA with two specific oligonucleotides: 5'-

20   GCGTCGACACCGTTTTTCCCCAGTAACCG-3' (containing a *Sal*I site) and 5'-

21   CGCGGATCCCATTGGAGCTTCGTTGAGCTG-3' (containing the *Bam*HI site) and

22   subcloned as a *Sal*I-*Bam*HI fragment into the pBI101.1 vector to obtain a translational

23   fusion.

D'Apuzzo 23 MPMI

1 **Confocal Analysis**

2 Confocal microscope analyses were performed using a Nikon PCM2000 (Bio-Rad,

3 Germany) laser scanning confocal imaging system. For GFP and RFP detection,

4 excitation was at 488 nm and detection between 515 and 530 nm. The images acquired

5 from the confocal microscope were processed using ImageJ bundle software

6 (http://rsb.info.nih.gov/ij/).

7 **Quantitative Real-time RT-PCR**

8 Total RNA was prepared from Lotus tissues using the procedure of Kistner and

9 Matamoros (2005). The samples were treated with DNAse I (Ambion) to remove

10 contaminating DNA the absence of which was subsequently confirmed by PCR. One

11 microgram of total RNA was annealed to random decamers and reverse-transcribed with

12 reverse transcriptase (Ambion) to obtain cDNA. Real time PCR was performed with a

13 DNA Engine Opticon 2 System, MJ Research (MA, USA) using SYBR to monitor

14 dsDNA synthesis. The ubiquitin (*UBI*) gene (AW719589) was used as an internal

15 standard. The concentration of primers was optimized for each PCR reaction and each

16 amplification was carried out in triplicate. The PCR program used was as follows: 95°C

17 for 13 min and 39 cycles of 94°C for 15 sec., 60°C for 15 sec. and 72°C for 15 sec. Data

18 were analyzed using Opticon Monitor Analysis Software Version 2.01 (MJ Research).

19 The qRT-PCR data were analyzed using comparative Ct method. The relative level of

20 expression was calculated with the following formula: relative expression ratio of the

21 gene of interest is $2^{-\Delta CT}$ with $\Delta CT = Ct_{AMT1}$ minus CT_{UBI}. Analysis of the melting curve

22 of PCR product at the end of the PCR run revealed a single narrow peak for each

23 amplification product, and fragments amplified from total cDNA were gel-purified and

D'Apuzzo 24 MPMI

1   sequenced to assure accuracy and specificity. The oligonucleotides used for the qRT-PCR

2   are the following: PII-forw 5'-GCAGAGGAAATGCCATGATT-3'; PII-rev 5'-

3   CACCACGGATTCCCATATTC-3';   CLERS2-forw   5'-

4   GCTCGTAATCTCCAAATCATTCACA-3';   CLERS2-rev   5'-

5   GGTGAGAGTCTTTGCTGTTGATATCC-3'

6   **SDS-PAGE and Western blot analysis**

7   Tissue powder from 0.5 g aliquots was prepared by grounding fresh tissue in liquid

8   nitrogen. The powder was then resuspended in 1 ml of 50 mM potassium phosphate

9   buffer, 10 mM☐2-Mercaptoethanol, 1 mM PMSF, pH 7.2 pre-chilled at 4°C. The cell-

10   free crude extract samples were centrifuged for 15 min at 12000 g to remove insoluble

11   material. Aliquots containing 20 μg protein from a given supernatant preparation were

12   separated by electrophoresis on a 12% (w/v) sodium dodecyl sulphate (SDS)

13   polyacrylamide gel. The separated proteins were then electroblotted onto polyvinylidene

14   fluoride (PVDF) membranes and rinsed with TBS (20 mM Tris-Hcl, 0.5 mM NaCl, pH

15   7.5). The membrane was stained with red ponceau to check for equal loaded amount of

16   proteins. PII protein was detected using the polyclonal antiserum raised against

17   recombinant *A. thaliana* PII protein (Ferrario-Mery et al. 2005). Western blot analysis

18   was done according to the manufacturer's instruction (ECL Plus Western Blotting

19   Detection System, Amersham, Uppsala, Sweden).

20   **Histochemical GUS Analysis**

21   Histochemical staining of whole plant and sections material was performed as described

22   by D'Apuzzo et al. (2004).

23   **Determination of Acetylene-Reduction Activity**

24

D'Apuzzo 25 MPMI

1   Detached roots with comparable number of nodules were placed in glass vials. The vials

2   were filled with an acetylene-air mixture (C_2H_2:air = 1:9 v/v). After 1 h of incubation at

3   25°C, the amount of ethylene in the gas phase was determined using a gas chromatograph

4   (PerkinElmer Clarus 580).

5   **Measurement of Polyamine Levels**

6   For polyamine extraction and HPLC analysis a benzoylation method was performed as

7   described previously (Flores and Galston, 1982; Smith and Davies, 1985) with some

8   modifications. 1 g of fresh tissue was homogenized in 10 mL of cold 0.2 N per-chloride

9   acid containing 1 µmol of hexanediamine as an internal standard. The samples are

10   incubated on ice for 40 min, and then centrifuged at 4°C for 20 min. Aliquots of 0.5 mL

11   of supernatant were added to 1 mL of 2 n NaOH with 10 µL of benzoyl chloride. The

12   mixtures were incubated at room temperature for 20 min, and the reaction was terminated

13   by the addition of 2 mL of saturated NaCl. Benzoylamines were extracted with 2 mL of

14   diethyl ether. After centrifugation, the ether layer was collected and dried under nitrogen

15   gas. The powdered samples were stored at -20°C until HPLC measurements. For HPLC

16   analysis, the residues were redissolved in 120 µL of methanol. Standards were treated in

17   a similar way with 1 µmol of putrescine, cadaverine, hexanediamine, spermidine, and

18   spermine in the reaction mixture. HPLC analysis was performed with a programmable

19   Kratos dual-pump liquid chromatograph with a detector 773. The solvent system

20   consisted of methanol and water, run at 65% (v/v) methanol at a flow rate of 0.7 mL/min.

21   Five microliters of benzoylated extracts was eluted at room temperature through a 4.6 3

22   250 mm, 5-mm particle size reverse-phase (C18) column (Varian, Walnut Creek, CA)

23   and detected at 254 mm. The peak areas were recorded on a pen recorder and calculated

24   by a computer with NIH Image software (National Institutes of Health, Bethesda, MD).

D'Apuzzo 26 MPMI

1 **Phylogenetic studies**

2 The evolutionary history was inferred using the Neighbor-Joining method (Saitou and

3 Nei 1987). The evolutionary distances were computed using the Poisson correction

4 method (Zuckerkandl and Pauling 1965) and are in the units of the number of amino acid

5 substitutions per site. The analyses involved 20 amino acid sequences. All positions

6 containing gaps and missing data were eliminated. Phylogenetic analyses were conducted

7 in MEGA5.2.2 (Tamura et al. 2007).

8 **Statistical analysis**

9 Statistical analyses were performed using the VassarStats ANOVA program available at:

10 http://faculty.vassar.edu/lowry/VassarStats.html

11

12 **Acknowledgements**

D'Apuzzo 27 MPMI

1 **Author contributions**

2 All the authors critically revised the article. E.D., V.V, A.P. and M.C. designed research;

3 E.D., A.P., V.V., S.O., A.B., M.S., M.L., A.R. performed research; V.V., S.E., M.C.

4 analyzed data; and M.C. wrote the paper.

5

6 **Literature cited**

7 Barbulova, A., D'Apuzzo, E., Rogato, A., and Chiurazzi, M. 2005. Improved procedures

8 for *in vitro* regeneration and for phenotypical analysis in the model legume *Lotus*

9 *japonicus.* Functional Plant Biology 32: 529-536.

10 Barbulova, A., Rogato, A., D'Apuzzo, E., Omrane, S., and Chiurazzi, M. 2007.

11 Differential effects of combined N sources on early steps of the Nod factor-dependent

12 transduction pathway in Lotus japonicus. Mol. Plant-Microbes Interact. 20: 994-1003.

13 Baud, S., Wuillème, S., To, A., Rochat, C., and Lepiniec, L. 2009. Role of WRINKLED1

14 in the transcriptional regulation of glycolitic and fatty acid biosynthetic genes in

15 Arabidopsis. The Plant Journal 60: 933-947.

16 Baud, S., Bourellier, A. B. F., Azzopardi, M., Berger, A., Dechorgnat, J., Daniel-Vedele,

17 F., Lepiniec, L., Miquel, M., Rochat, C., Hodges, M., and Ferrario-Mery, S. 2010. PII is

18 induced by WRINKLED1 and fine-tunes fatty acid composition in seeds of Arabidopsis

19 thaliana. The Plant Journal 64: 291-303.

20 Beez, S. Fokina, O. Herrmann, C. and Forchhammer, K. (2009) N-Acetyl-L-Glutamate

21 kinase (NAGK) from oxygenic phototrophs: P(II) signal transduction across domains of

22 life reveals novel insights in NAGK control. J. Mol. Biol. 389: 748–758.

D'Apuzzo 28 MPMI

1   Bisseling, T., van den Bos, R.C., and van Kammen, A. 1978. The effect of ammonium

2   nitrate on the synthesis of nitrogenase and the concentration of leghemoglobin in pea root

3   nodules induced by Rhizobium leguminosarum. Biochim. Biophys. Acta 539: 1-11.

4   Boscari, A., del Giudice, J., Ferrarini, A., Venturini, L., Zaffini, A. L., Delledonne, M.,

5   and Puppo, A. 2013. Expression dynamics of the Medicago truncatula transcriptome

6   during the symbiotic interaction with Sinorhizobium meliloti: which role for nitric oxide?

7   Plant Physiol. 161: 425-439.

8   Burillo, S., Luque, I., Fuentes, I., and Contreras, A. 2004. Interactions between the

9   nitrogen signal transduction protein PII and N-acetyl glutamate kinase in organisms that

10 perform oxygenic photosynthesis. J. Bacteriol 186: 3346-3354.

11 Caetano-Anollés, G., and Gresshoff, P.M. 1991. Plant genetic control of nodulation. Ann.

12 Rev. Microbiol. 45: 345-382.

13 Cheah, E., Carr, P. D., Suffolk, P. M., Vasudevan, S. G., Dixon, N. E., and Ollis, D. L.

14 1994. Structure of the Escherichia coli signal transducing protein PII. Structure 2: 981-

15 990.

16 Chen, Y. M., Ferrar, T. S., Lohmeir-Vogel, E., Morrice, N., Mizuno, Y., Berenger, B.,

17 Ng, K. K. S., Muench, D.G., and Moorhead, G.B.G. 2006. The PII signal transduction

18 protein of Arabidopsis thaliana forms an arginine-regulated complex with plastid N-

19 acetyl glutamate kinase. J. Biol. Chem. 281: 5726-5733.

20 Complainville, A., Brocard, L., Roberts, I., Dax, E., Sever, N., Sauer, N., Kondorosi, A.,

21 Wolf, S., Oparka, K., and Crespi, M. 2003. Nodule initiation involves the creation of a

22 new symplasmic field in specific root cells of medicago species. Plant Cell 120: 2778-

23 2791.

D'Apuzzo 29 MPMI

D'Apuzzo, E., Rogato, A., Simon-Rosin, U., El Alaoui, H., Barbulova, A., Betti, M., Dimou, M., Katinakis, P., Marquez, A., Marini, A. M., Udvardi, K. M., and Chiurazzi, M. 2004. Characterisation of three functional high affinity ammonium transporters in *Lotus japonicus* with differential transcriptional regulation and spatial expression. Plant Physiol. 134: 1763-1774.

Del Giudice, J., Cam, Y., Damiani, I., Fung-Chat, F., Meilhoc, E., Bruand, C., Brouquisse, R., Puppo, A., and Boscari, A. 2011. Nitric oxide is required for an optimal establishment of the Medicago truncatula-Sinorhizobium meliloti symbiosis. New Phytologist 191: 405-417.

Duby, G., Oufattole, M., and Boutry, M. 2001. Hydrophobic residues within the predicted N-terminal amphiphilic a-helix of a plant mitochondrial targeting presequence play a major role in *in vivo* import. The Plant Journal 27: 539-549.

Efrose, R. C., Flemetakis, E., Sfichi, L., Stedel, C., Kouri, E. D., Udvardi, M. K., Kotzabasis, K., and Katinakis, P. 2008. Characterization of spermidine and spermine synthases in Lotus japonicus: induction and spatial organization of polyamine biosynthesis in nitrogen fixing nodules. Planta 228: 37-49.

Feria Bourrellier, A. B., Valot, B., Guillot, A., Ambard-Bretteville, F., Vidal, J., and Hodges, M. 2010. Chloroplast acetyl-CoA carboxylase activity is 2-oxoglutarate–regulated by interaction of PII with the biotin carboxyl carrier subunit. Proc. Natl. Acad. Sci. U.S.A. 107: 502-507.

Ferrario-Mèry, S., Bouvet, M., Leleu, O., Savino, G., Hodges, M., and Meyer, C. 2005. Physiological characterization of Arabidopsis mutants affected in the expression of the

D'Apuzzo 30 MPMI

1   putative regulatory protein PII. Planta 223: 28-39.

2   Ferrario-Mèry, S., Besin, E., Pichon, O., Meyer, C., and Hodges, M. 2006. The regulatory

3   PII protein controls arginine biosynthesis in Arabidopsis. F.E.B.S. Letters 580: 2015-

4   2010.

5   Flemetakis, E., Efrose, R. C., Desbrosses, G., Dimou, M., Delis, C., Aivalakis, G.,

6   Udvardi, M. K., and Katinakis, P. 2004. Induction and spatial organization of polyamine

7   biosynthesis during nodule development in Lotus japonicus. Mol. Plant. Microbes

8   Interact. 17: 1283-1293.

9   Flores, H. E., and Galston, A. W. 1982. Analysis of polyamines in higher plants by high

10   performance liquid cromatography. Plant Physiol. 69: 701-706.

11   Forchhammer, K. 2004. Global carbon/nitrogen control by PII signal transduction in

12   cyanobacteria: from signals to targets. F.E.M.S. Microbiol. 28: 319-333.

13   Forchhammer, K. 2008. P(II) signal transducers: novel functional and structural insights.

14   Trends Microbiol. 16: 65-72.

15   Fujihara, S., Abe, H., Minakawa, Y., Akao, S., and Yoneyama, T. 1994. Polyamines in

16   nodules from various plant-microbe symbiotic associations. Plant Cell Physiol. 35: 1127-

17   1134.

18   Gamborg, O. L. 1970. The effects of amino acids and ammonium on the growth of plant

19   cells in suspension culture. Plant Physiol. 45:372-375.

20   Hajdukiewicz, P., Svab, Z., and Maliga, P. 1994. The small, versatile pPZP family of

21   Agrobacterium binary vectors for plant transformation. Plant Mol. Biol. 25: 989-94.

D'Apuzzo 31 MPMI

1   Hsieh, M. H., Lam, H. M., Van de Loo, F. J., and Coruzzi, G. 1998. A PII-like protein in

2   Arabidopsis: Putative role in nitrogen sensing. Proc. Natl. Acad. Sci. U.S.A. 95: 13965-

3   13970.

4   Huergo, L. F., Chandra, G., and Merrick, M. 2013. P(II) signal transduction proteins:

5   nitrogen regulation and beyond. F.E.M.S. Microbiol. Rev. 37: 251-83.

6   Jefferson, R.A. 1987. Assaying chimeric genes in plants: The GUS gene fusion system.

7   Plant Mol. Biol. Rep. 5: 387-405.

8   Jeudy, C., Ruffel, S., Freixes, S., Tillard, P., Santoni, A.L., Morel, S., Journet, E.P., Duc,

9   G., Gojon, A., Lepetit, M., and Salon, C. 2010. Adaptation of Medicago truncatula to

10   nitrogen limitation is modulated via local and systemic nodule developmental responses.

11   New Phytologist 185: 817-828.

12   Jiang, P., and Ninfa, A. J. 2007. Escherichia coli PII signal transduction protein

13   controlling nitrogen assimilation acts as a sensor of adenylate energy charge in vitro.

14   Biochemistry 46: 12979-12996.

15   Kistner, C., and Matamoros, M. 2005. RNA isolation using phase extraction and LiCl

16   precipitation. Lotus japonicus handbook. Edited by Marquez, A.J. Springer Verlag.

17   Dordrecht press. pp 123-124.

18   Kohler, R. H. Cao, J. Zipfel, W. R. Webb, W. W. and Hanson, M. R. (1997) Exchange of

19   protein molecules through connections between higher plant plastids. *Science* 276: 2039-

20   2042.

21   Maeo, K., Tokuda, T., Ayame, A., Mitsui, N., Kawai, T., Tsukagoshi, H., Ishiguro, S.,

22   and Nakamura, K. 2009. An AP-type transcription factor, WRINKLED1, of Arabidopsis

D'Apuzzo 32 MPMI

1 thaliana binds to the AW-box sequence conserved among proximal upstream regions of

2 genes involved in fatty acid synthesis. The Plant Journal 60: 476-487.

3 Martirani, L., Stiller, J., Mirabella, R., Alfano, F., Lamberti, A., Radutoiu, S. E.,

4 Iaccarino, M., Gressohff, P. M., and Chiurazzi, M. 1999. Establishment of a T-DNA

5 Tagging Program in the Model Legume *Lotus Japonicus* . Expression patterns, activation

6 frequencies and potential for insertional mutagenesis. Molecular Plant Microbe Interact.

7 12: 275-284.

8 Maheswaran, M., Urbanke, C., and Forchhammer, K. 2004. Complex formation and

9 catalytic activation by the PII signaling protein of N-acetyl-L-glutamate ginase from

10 *Synechococcus elongatus* strain PCC7942. J. Biol. Chem. 279: 55202-55210.

11 Matamoros, M.A., Baird, L. M., Escuredo, P. R., Dalton, D. A., Minchin, F. R., Iturbe-

12 Ormaetxe, I., Rubio, M. C., Moran, J. F., Gordon, A.J., and Becana, M. 1999. Stress-

13 induced legume root nodule senescence. Physiological, biochemical, and structural

14 alterations. Plant Physiol. 121: 97-112.

15 Mishima, E., Hosokawa, A., Imaizumi-Anraku, H., Saito, K., Kawaguchi, M., and Saeki,

16 K. 2008. Requirement for Mesorhizobium loti ornithine transcarbamoylase for successful

17 symbiosis with Lotus japonicus as revealed by an unexpected long-range genome

18 deletion. Plant Cell Physiology 49: 301-313.

19 Mizuno, Y., Berenger, B., Moorhead, G. B., and Ng, K. K. 2007a. Crystal structure of

20 Arabidopsis PII reveals novel structural elements unique to plants. Biochemistry 46:

21 1477-1483.

D'Apuzzo 33 MPMI

1 Mizuno, Y., Moorhead, G. B., and Ng, K. K. 2007b. Structural basis for the regulation of

2 N-acetylglutamate kinase by PII in Arabidopsis thaliana. Journal of Biol. Chem. 282:

3 35733-35740.

4 Moorhead, G. B. G., and Smith, C. S. 2003. Interpreting the plastid carbon, nitrogen, and

5 energy status. A role for PII? Plant Physiol. 133: 492-498.

6 Omrane, S., Ferrarini, A., D'Apuzzo, E., Rogato, A., Delledonne, M., and Chiurazzi, M.

7 2009. Symbiotic competence in Lotus japonicus is affected by plant nitrogen status:

8 transcriptomic identification of genes affected by a new signalling pathway. New

9 Phytologist 183: 380-394.

10 Omrane, S., and Chiurazzi, M. 2009. A variety of regulatory mechanisms are involved in the

11 nitrogen-dependent modulation of the nodule organogenesis program in legume roots.

12 Plant Signaling and Behavior 4: 1066-1068.

13 Okamoto, S., Ohnishi, E., Sato, S., Takahashi, H., Nakazono, M., Tabata, S., and

14 Kawaguchi, M. 2009. Nod factor/nitrate-induced CLE genes that drive HAR1-mediated

15 systemic regulation of nodulation. Plant & Cell Physiology 50: 67-77.

16 Okamoto, S., Shinohara, H., Mori, T., Matsubayashi Y., and Kawaguchi, M. 2013. Root-

17 derived CLE glycopeptides control nodulation by direct binding to HAR1 receptor

18 kinase. Nat. Commun. 4: 2191.

19 Pathirana, A. M., Vance, C. P., Miller, S. S., and Gantt, S. 1992. Alfalfa root nodule

20 phosphoenolpiruvate carboxylase: characterization of the cDNA and expression in

21 effective and plant-controlled ineffective nodules. Plant Mol. Biol. 20:437-450.

22 Pauly, N., Ferrari, C., Andrio, E., Marino, D., Piardi, S., Brouquisse, R., Baoudoin, E.,

23 and Puppo, A. 2011. MtNOA1/RIF modulates Medicago truncatula-Sinorhizobium

D'Apuzzo 34 MPMI

1 meliloti nodule development without affecting its nitric oxide content. J. of Experim.

2 Botany 62: 939-948.

3 Radchenko, M. V., Thornton, J., and Merrick, M. 2013. P(II) signal transduction proteins

4 are ATPases whose activity is regulated by 2-oxoglutarate. Proc. Natl. Acad. Sci. U.S.A.

5 110: 12948-12953.

6 Ruffel, S., Freixes, S., Balzergue, S., Tillard, P., Jeudy, C., Martin-Magniette, M. L., van

7 der Merwe, M. J., Kakar, K., Gouzy, J., Fernie, A. R., Udvardi, M., Salon, C., Gojon, A.,

8 and Lepetit, M. 2008. Systemic signaling of the plant nitrogen status triggers specific

9 transcriptome responses depending on the nitrogen source in Medicago truncatula. Plant

10 Physiol. 146: 2020-2035.

11 Sant'anna, F. H., Trentini, D.B., de Souto-Weber, S., Cecagno, R., Ceroni da Silva, S.,

12 and Schrank, I. S. 2009. The PII superfamily revised: a novel group and evolutionary

13 insights. J. Mol. Evol. 68: 322-336.

14 Schulze, J., Shi, L., Blumenthal, J., Samac, D. A., Gantt, J. S., Vance, J. P. 1998.

15 Inhibition of alfalfa root nodule phosphoenolpyruvate carboxylase through an antisense

16 strategy impacts nitrogen fixation and plant growth. Phytochemistry 49:341-346.

17 Smith, C. S., Welji, A. M., and Moorhead, G. B. G. 2003. Molecular properties of the

18 putative nitrogen sensor PII from Arabidopsis thaliana. The Plant Journal 33: 353-360.

19 Smith, M. A., and Davies, P. J. 1985. Separation and quantitation of polyamines in plant

20 tissue by high performance liquid chromatography of their dansyl derivatives. Plant

21 Physiol. 78: 89-91.

D'Apuzzo 35 MPMI

1 Smith, C. S., Morrice, N. A., Moorhead, G. B. G. 2004. Lack of evidence for

2 phosphorylation of Arabidopsis thaliana PII: implications for plastid carbon and nitrogen

3 signaling. Biochimica et Biophysica Acta 1699: 145-154.

4 Saitou, N., and Nei, M. 1987. The Neighbor-Joining method: A new method for

5 reconstructing phylogenetic trees. Molecular Biology and Evolution 4: 406-425.

6 Sugiyama, K., Hayakawa, T., Kudo, T., Ito, T., and Yamaya, T. 2004. Interaction of N-

7 acetylglutamate kinase with a PII-like protein in rice. Plant Cell Physiol. 45: 1768-1778.

8 Tamura, K., Dudley, J., Nei, M., and Kumar, S. 2007. MEGA4: Molecular Evolutionary

9 Genetics Analysis (MEGA) software version 4.0. Mol. Biol. and Evol. 24: 1596-1599.

10 Terakado, J., Yoneyama, T., and Fujihara, S. 2005. Shoot-applied polyamines suppress

11 nodule formation in soybean (Glycine max). Journal of Plant Physiol. 163: 497-505.

12 Tsikou, D., Kallionati, C., Fotelli, M. N., Nikolopoulos, D., Katinakis, P., Udvardi, M.

13 K., Rennenberg, H., and Flemetakis, E. 2013. Cessation of photosynthesis in Lotus

14 japonicus leaves leads to reprogramming of nodule metabolism. Journal of Experimental

15 Botany 64: 1317-1332.

16 Uhrig, R. G., Kenneth, K. S., Ng, K. K., and Moorhead, G. B. G. 2009. PII in higher

17 plants: a modern role for an ancient protein. Trends in Plant Science 14: 505-511.

18 Vance, C. P. 2008. Carbon and Nitrogen metabolism in legume nodules. In Nitrogen-

19 fixing leguminous symbioses. Edited by Dilworth, M.J., James, E.K., Sprent, J.I.,

20 Newton, W. E, Springer Netherlands, Kluwer Academic Publishers pp 293-320.

21 Vasudevan, S. G., Gedye, C., Dixon, N. E., Cheah, E., Carr, P. D., Suffolk, P. M., Jeffrey,

22 P. D., and Ollis, D. L. 1994. Escherichia coli PII protein: purification, crystallisation and

23 oligomeric structure. F.E.B.S. Lett. 337: 255-258.

D'Apuzzo 36 MPMI

1   Wisniewski, J. P., and Brewin, N. J. 2000. Construction of transgenic Pea lines with

2   modified expression of diamine oxidase and modified nodulation responses with

3   exogenous putrescine. Mol. Plant Micr. Inter. 13: 922-928.

4   Zeth, K., Fokina, O., and Forchhammer, K. 2014. Structural basis and target-specific

5   modulation of ADP sensing by the Synechococcus elongatus PII signaling protein. The

6   Journal of Biological Chemistry 289: 8960-8972.

7   Zhang, H., Jennings, A., Barlow, P.W., and Forde, B.G. 1999. Dual pathways for

8   regulation of root branching by nitrate. Proc. Natl. Acad. Sci. U.S.A. 96: 6529-6534.

9   Zuckerkandl, E., and Pauling, L. 1965. Evolutionary divergence and convergence in

10 proteins, in Evolving Genes and Proteins. Edited by Bryson, V., and Vogel, H.J.

11 Academic Press, New York, pp 97-166.

12

13

14

15

16

17

18

19

20

21

22

23

D'Apuzzo 37 MPMI

1 **Legend to figures**

2 **Figure 1**

3 Phylogenetic relationship of PII amino acid sequences. Twenty full length amino acid

4 sequences were aligned with the ClustalW program. The optimal tree with the sum of

5 branch length = 2.33470189 is shown. The tree is drawn to scale, with branch lengths in

6 the same units as those of the evolutionary distances used to infer the phylogenetic tree.

7 The evolutionary distances were computed using the Poisson correction method

8 (Zuckerkandl and Pauling 1965) and are in the units of the number of amino acid

9 substitutions per site. Phylogenetic analyses were conducted in MEGA5.2.2 (Tamura et

10 al. 2007). Protein sequences were obtained from NCBInr (**www.ncbi.nlm.nih.gov**) and

11 DOEJGI (**http://jgi.doe.gov**) online databases using BLSTP algorithms. Sequences are as

12 follows: *Arabidopsis thaliana, Cajanus cajan, Capsella rubella, Chlamydomonas*

13 *reinhardtii, Cicer arietinum, Escherichia coli, Fragaria vesca, Glycine max, Medicago*

14 *sativa, Medicago truncatula, Oryza sativa, Phaseolus vulgaris, Physcomitrella patens,*

15 *Populus trichocarpa, Porphyra purpurea, Prunus persica, Solanum lycopersicon, Vitis*

16 *vinifera, Synechococcus sp.* PCC7002.

17 **Figure 2.**

18 *LjGLB1* transcriptional regulation in different organs and during day-night cycle. A:

19 expression in different organs. RNAs were extracted by 3 weeks old plants grown on

20 1mM NH_4NO_3 (+N) or without nitrogen (-N). White bars, roots; black bars, leaves; grey

21 bar, nodules. B-C. Expression during the day-night cycle. Plants were grown in

22 hydroponic conditions (1mM NH_4NO_3) and RNAs were extracted by roots (B) and leaves

23 (C) of 3 weeks old plants at different hours from the beginning of light (white) and dark

D'Apuzzo 38 MPMI

1 (grey) period. The presence of 3% sucrose in the growth medium is indicated. *LjGLB1*

2 expression levels were normalized with respect to the internal control ubiquitin (*UBI*)

3 gene and plotted relative to the expression from roots in A and to the 7 hours dark

4 samples in B and C. Data bars represent the mean and standard deviations of data

5 obtained with RNA extracted from three different sets of plants and 3 real-time qPCR

6 experiments. Asterisks indicate significant differences with the levels of expression under

7 light conditions ($P < 0.05$).

8 **Figure 3.**

9 Effect of N deficiency treatment on *LjGLB1* and *LjAMT1;1* expression. RNAs were

10 extracted from roots of plants grown in presence of 1mM NH_4NO_3 (T0) and after shifting

11 to -N conditions (24hrs/T1, 48 hrs/T2, 72 hrs/T3, 5 days/T4). Expression levels were

12 normalized with respect to the internal control ubiquitin (*UBI*) gene (see Material and

13 Methods) and plotted relative to the expression of T0. White bars: *LjGLB1*; black bars:

14 *LjAMT1;1*. Data bars represent the mean and standard deviations of data obtained with

15 RNA extracted from three different sets of plants and 3 real-time PCR experiments.

16 Asterisks indicate significant differences with T0 conditions ($P < 0.05$).

17 **Figure 4.**

18 Spatial profile of expression of the *LjGLB1* gene in root and nodular tissues.

19 A-C: whole mount staining of *L. japonicus* hairy roots transformed with the *pLjGLB1-*

20 *gus*A construct. A: GUS activity in the root vascular bundle; B and C: GUS activity in the

21 root vascular bundle, cortical cells and root cap (arrows); D: cross section of a transgenic

22 root with GUS activity detected into the root stele; E: longitudinal section of a transgenic

D'Apuzzo 39 MPMI

1 mature representative nodule. GUS activity is detected in the nodule vascular bundle

2 (arrows) and parenchyma (arrowhead). Bars on the left = 50 μm.

3 **Figure 5.**

4 Molecular characterization of 35S-*LjGLB1* over-expressing lines. A: semi-quantitative

5 analysis of *GLB1* transcript level in roots of wild type (white bar) and the two

6 overexpressing lines 7-13 and 8-9 (T2 homozigous plants; black bars). Expression levels

7 were normalized with respect to the internal control ubiquitin (*UBI*) gene and plotted

8 relative to the expression in wild type plants. Data bars represent the mean and standard

9 deviations of data obtained with RNA extracted from two different sets of plants and 3

10 RT-PCR experiments. B: The corresponding analysis of PII protein levels by western blot

11 using *A. thaliana* PII specific antibody. The lanes contain 20 □g of soluble proteins

12 extracted from three Lotus plants. Asterisks indicate significant differences with the level

13 of expression in wild type plants (P<0.05).

14 **Figure 6**

15 Nodular phenotypical analysis of wild type and PII over-expressing plants grown in low

16 N conditions. A. Number of nodules per plant. Plants were germinated on H_2O agar, and

17 7 days old seedlings transferred on Gamborg B5 derived medium with 10 μM NH_4KNO_3

18 as sole N source and inoculated with *M. loti*. Nodules were scored at 4 weeks after

19 inoculation. Wild type (white bars); 8.9 (black bars); 7.13 (grey bar). Data represent the

20 mean and standard error obtained from three independent experiments (15 plants per

21 experiment). Asterisks indicate significant differences with the number of nodules

22 observed without putrescine. B. Acetylene Reduction Activity (ARA) per nodule weight

23 of wild type and 8-9 plants. Data bars indicate the mean and standard error of three

1   independent experiments (n=2 plants per exp.) Asterisk indicates significant difference

2   (p<0.02). C. Spermine (left) and spermidine (right) content in nodules of wild type and 8-

3   9 plants. Polyamines were extracted from 4 weeks old nodules. Data represent the mean

4   and standard error obtained from two independent experiments (20 plants per

5   experiment). Asterisk indicates significant difference (p<0.01). D. Citrulline content in

6   nodules of wild type and 8-9 plants. Polyamines were extracted from 4 weeks old

7   nodules. Data represent the mean and standard error obtained from two independent

8   experiments (20 plants per experiment). Asterisk indicates significant difference

9   (p<0.01).

10   **Figure 7**

11   N-dependent nodule formation phenotypes in wild type and *L. japonicus* PII over-

12   expressing 7-13 and 8-9 plants. A. White bars represent number of nodules observed in

13   plants pre-incubated 10 days on 10 μM NH_4NO_3 and then shifted on the same conditon

14   and inoculated with *M. loti*. Black bars represent nodule numbers observed in plants pre-

15   incubated 10 days on 10 mM NH_4NO_3 and then shifted on 10 μM NH_4NO_3 and

16   inoculated with *M. loti*. Nodules were counted at 4 weeks post inoculation. Data represent

17   the mean and standard error obtained from three independent experiments (20 plants per

18   experiment). Asterisks indicate significant differences with the number of nodules

19   observed in wild type plants pre-incubated on 10 mM NH_4NO_3 (P<0.05). B. Relative

20   quantification of *LjCLERS2* mRNA measured by qRT-PCR in roots of wild type and 8-9

21   plants incubated 10 days on 10 mM NH_4NO_3 or 10 μM NH_4NO_3 conditions. *L. japonicus*

22   *UBI* was used as reference gene to normalize the expression of *LjCLERS2*. Data bars

23   represent means and SD of data obtained with RNA extracted from two different sets of

D'Apuzzo 41 MPMI

1   plants and three technical repeats. Asterisks indicate significant differences with the level

2   of expression in 10 mM conditions (P<0.05).

3   **Figure 8**

4   Pathways of polyamines biosynthesis. The dotted lines indicate the putative nitric oxide

5   synthase-dependent pathway for NO biosynthesis.

6

7   **Legend to supplementary figures**

8   **Figure S1**

9   Intron/exon organization of the *LjGLB1* gene. Numbers above exons (black boxes) and

10   below introns (lines) indicate their length in nucleotides. The positions of the start (ATG)

11   and stop (TGA) codons are indicated. The amino acid sequence of the *L. japonicus* PII

12   protein is shown at the bottom.

13   **Figure S2.**

14   Subcellular localization of the PII protein. Confocal laser scanning micrographs of *L.*

15   *japonicus* hairy roots stably expressing the 35S-*LjGLB1*-GFP (A) and *AtrecA*-DsRed2

16   (B) fusions. In the merged image (C) the co-localized signals of green GFP and red

17   DsRed2 fluorescence appears yellow. Bar = 50 μm.

18   **Figure S3**

19   Time course of the *LjGLB1* transcriptional regulation in root and nodules tissues after *M.*

20   *loti* inoculation. RNAs were extracted from roots of seedlings grown in presence of

21   10□M NH$_4$NO$_3$ (T0) and at different times after inoculation (24 hrs, 72 hrs) and from

22   young (12 days) and mature nodules (28 days). Expression levels were normalized with

23   respect to the internal control ubiquitin (*UBI*) gene and plotted relative to the expression

D'Apuzzo 42 MPMI

1 of T0. Data bars represent the mean and standard deviations of data obtained with RNA

2 extracted from three different sets of plants and 3 real-time PCR experiments.

3 **Figure S4**

4 **A,** 60 □m thick sections of representative four weeks old nodules of wild type and 8-9

5 plants. No differences are observed in nodule diameter and density of invaded cells. **B,**

6 Fresh shoot weigth of wild type, 7.13 and 8-9 plants four weeks after inoculation. Plants

7 were germinated on H_2O agar, and 7 days old seedlings transferred on Gamborg B5

8 derived medium with 10 μM NH_4KNO_3 as sole N source and inoculated with *M. loti*.

9 Data represent the mean and standard error obtained from three independent experiments

10 (15 plants per experiment).

11
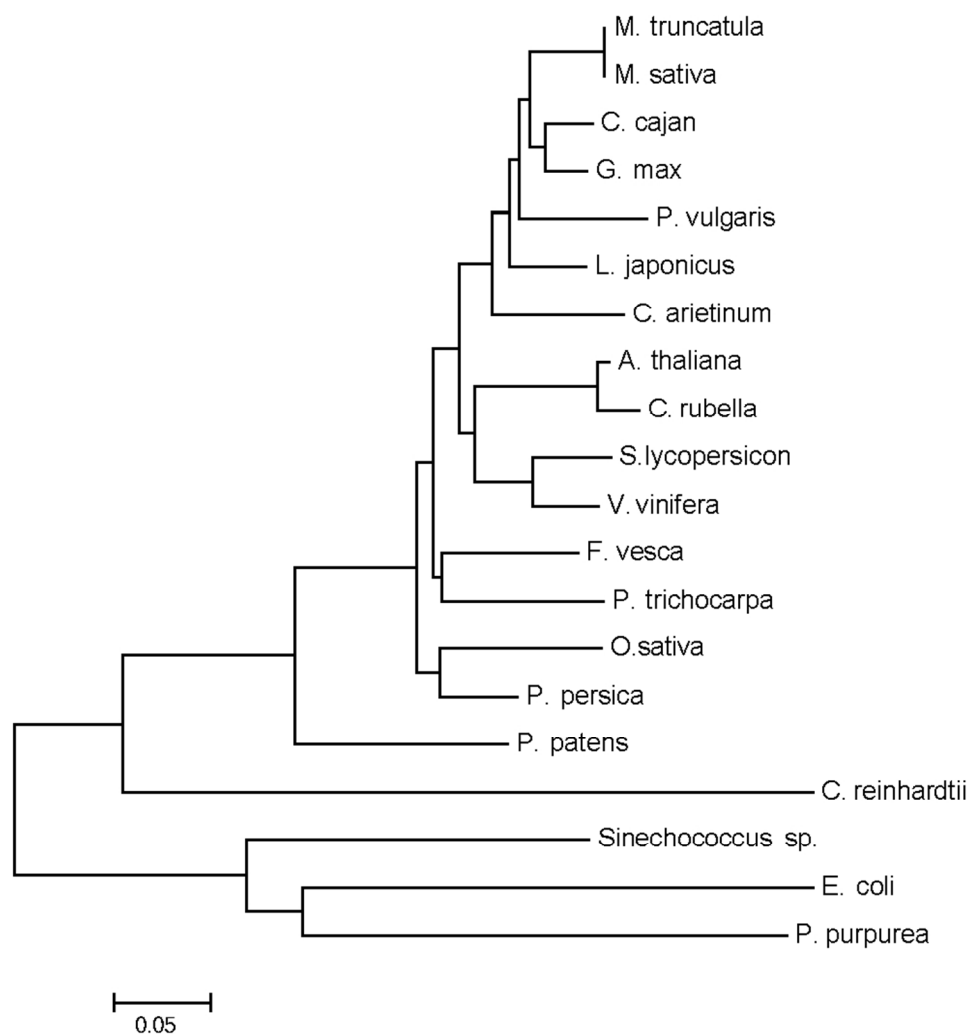
Phylogenetic relationship of PII amino acid sequences. Twenty full length amino acid sequences were aligned with the ClustalW program. The optimal tree with the sum of branch length = 2.33470189 is shown. The tree is drawn to scale, with branch lengths in the same units as those of the evolutionary distances used to infer the phylogenetic tree. The evolutionary distances were computed using the Poisson correction method (Zuckerkandl and Pauling 1965) and are in the units of the number of amino acid substitutions per site. Phylogenetic analyses were conducted in MEGA5.2.2 (Tamura et al. 2007). Protein sequences were obtained from NCBInr (www.ncbi.nlm.nih.gov) and DOEJGI (http://jgi.doe.gov) online databases using BLSTP algorithms. Sequences are as follows: Arabidopsis thaliana, Cajanus cajan, Capsella rubella, Chlamydomonas reinhardtii, Cicer arietinum, Escherichia coli, Fragaria vesca, Glycine max, Medicago sativa, Medicago truncatula, Oryza sativa, Phaseolus vulgaris, Physcomitrella patens, Populus trichocarpa, Porphyra purpurea, Prunus persica, Solanum lycopersicon, Vitis vinifera, Synechococcus sp. PCC7002.
131x141mm (200 x 200 DPI)
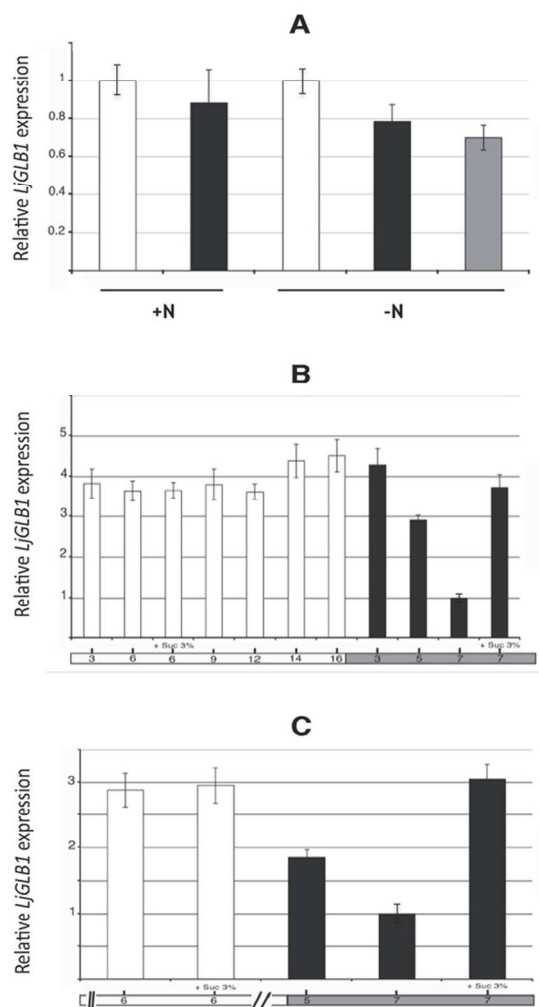
LjGLB1 transcriptional regulation in different organs and during day-night cycle. A: expression in different organs. RNAs were extracted by 3 weeks old plants grown on 1mM NH4NO3 (+N) or without nitrogen (-N). White bars, roots; black bars, leaves; grey bar, nodules. B-C. Expression during the day-night cycle. Plants were grown in hydroponic conditions (1mM NH4NO3) and RNAs were extracted by roots (B) and leaves (C) of 3 weeks old plants at different hours from the beginning of light (white) and dark (grey) period. The presence of 3% sucrose in the growth medium is indicated. LjGLB1 expression levels were normalized with respect to the internal control ubiquitin (UBI) gene and plotted relative to the expression from roots in A and to the 7 hours dark samples in B and C. Data bars represent the mean and standard deviations of data obtained with RNA extracted from three different sets of plants and 3 real-time qPCR experiments. Asterisks indicate significant differences with the levels of expression under light conditions (P<0.05).
91x105mm (300 x 300 DPI)
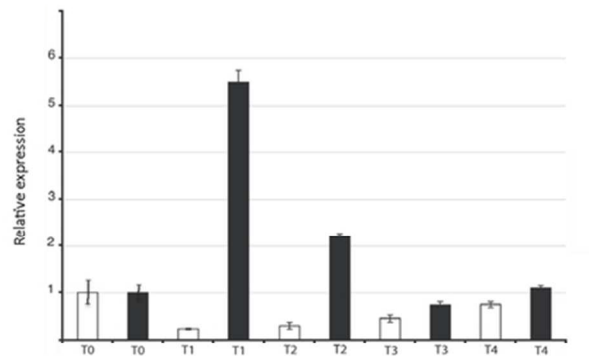
Effect of N deficiency treatment on LjGLB1 and LjAMT1;1 expression. RNAs were extracted from roots of plants grown in presence of 1mM NH4NO3 (T0) and after shifting to -N conditions (24hrs/T1, 48 hrs/T2, 72 hrs/T3, 5 days/T4). Expression levels were normalized with respect to the internal control ubiquitin (UBI) gene (see Material and Methods) and plotted relative to the expression of T0. White bars: LjGLB1; black bars: LjAMT1;1. Data bars represent the mean and standard deviations of data obtained with RNA extracted from three different sets of plants and 3 real-time PCR experiments. Asterisks indicate significant differences with T0 conditions (P<0.05).
59x44mm (300 x 300 DPI)
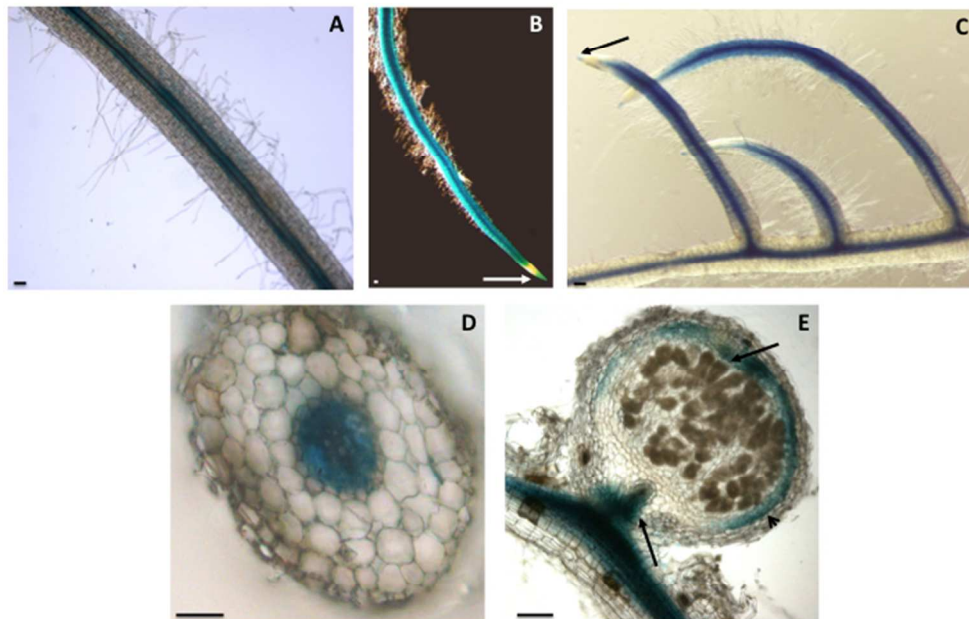
Spatial profile of expression of the LjGLB1 gene in root and nodular tissues.
A-C: whole mount staining of L. japonicus hairy roots transformed with the pLjGLB1-gusA construct. A: GUS activity in the root vascular bundle; B and C: GUS activity in the root vascular bundle, cortical cells and root cap (arrows); D: cross section of a transgenic root with GUS activity detected into the root stele; E: longitudinal section of a transgenic mature representative nodule. GUS activity is detected in the nodule vascular bundle (arrows) and parenchyma (arrowhead). Bars on the left = 50 μm.

254x190mm (72 x 72 DPI)
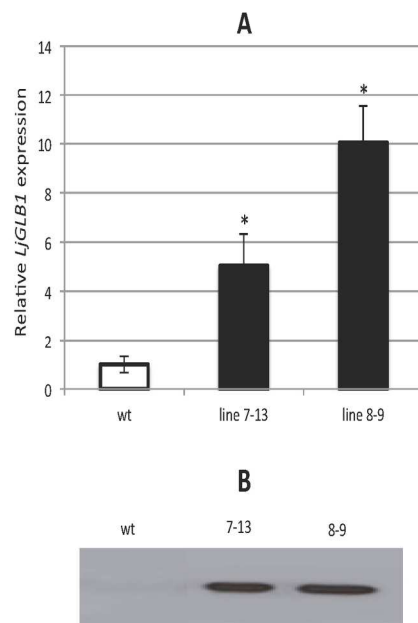
Molecular characterization of 35S-LjGLB1 over-expressing lines. A: semi-quantitative analysis of GLB1 transcript level in roots of wild type (white bar) and the two overexpressing lines 7-13 and 8-9 (T2 homozigous plants; black bars). Expression levels were normalized with respect to the internal control ubiquitin (UBI) gene and plotted relative to the expression in wild type plants. Data bars represent the mean and standard deviations of data obtained with RNA extracted from two different sets of plants and 3 RT-PCR experiments. B: The corresponding analysis of PII protein levels by western blot using A. thaliana PII specific antibody. The lanes contain 20 μg of soluble proteins extracted from three Lotus plants. Asterisks indicate significant differences with the level of expression in wild type plants (P<0.05).
190x198mm (300 x 300 DPI)
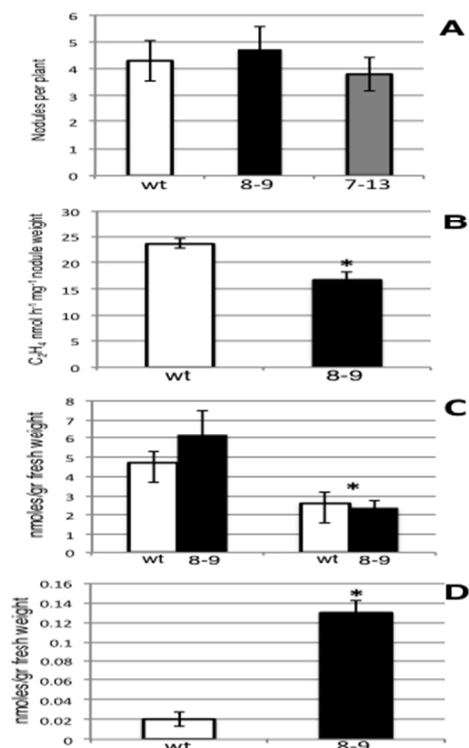
Nodular phenotypical analysis of wild type and PII over-expressing plants grown in low N conditions. A. Number of nodules per plant. Plants were germinated on H2O agar, and 7 days old seedlings transferred on Gamborg B5 derived medium with 10 µM NH4KNO3 as sole N source and inoculated with M. loti. Nodules were scored at 4 weeks after inoculation. Wild type (white bars); 8.9 (black bars); 7.13 (grey bar). Data represent the mean and standard error obtained from three independent experiments (15 plants per experiment). Asterisks indicate significant differences with the number of nodules observed without putrescine. B. Acetylene Reduction Activity (ARA) per nodule weight of wild type and 8-9 plants. Data bars indicate the mean and standard error of three independent experiments (n=2 plants per exp.) Asterisk indicates significant difference (p<0.02). C. Spermine (left) and spermidine (right) content in nodules of wild type and 8-9 plants. Polyamines were extracted from 4 weeks old nodules. Data represent the mean and standard error obtained from two independent experiments (20 plants per experiment). Asterisk indicates significant difference (p<0.01). D. Citrulline content in nodules of wild type and 8-9 plants. Polyamines were extracted from 4 weeks old nodules. Data represent the mean and standard error obtained from two independent experiments (20 plants per experiment). Asterisk indicates significant difference (p<0.01).
254x190mm (72 x 72 DPI)
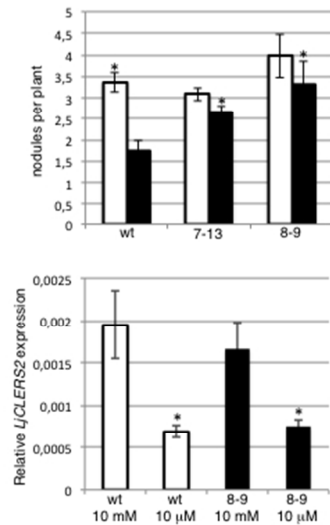
N-dependent nodule formation phenotypes in wild type and L. japonicus PII over-expressing 7-13 and 8-9 plants. A. White bars represent number of nodules observed in plants pre-incubated 10 days on 10 µM NH4NO3 and then shifted on the same conditon and inoculated with M. loti. Black bars represent nodule numbers observed in plants pre-incubated 10 days on 10 mM NH4NO3 and then shifted on 10 µM NH4NO3 and inoculated with M. loti. Nodules were counted at 4 weeks post inoculation. Data represent the mean and standard error obtained from three independent experiments (20 plants per experiment). Asterisks indicate significant differences with the number of nodules observed in wild type plants pre-incubated on 10 mM NH4NO3 (P<0.05). B. Relative quantification of LjCLERS2 mRNA measured by qRT-PCR in roots of wild type and 8-9 plants incubated 10 days on 10 mM NH4NO3 or 10 µM NH4NO3 conditions. L. japonicus UBI was used as reference gene to normalize the expression of LjCLERS2. Data bars represent means and SD of data obtained with RNA extracted from two different sets of plants and three technical repeats. Asterisks indicate significant differences with the level of expression in 10 mM conditions (P<0.05).
254x190mm (72 x 72 DPI)
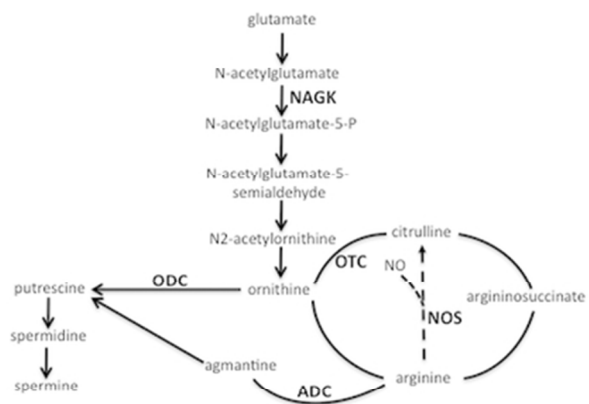
Pathways of polyamines biosynthesis. The dotted lines indicate the putative nitric oxide synthase-dependent pathway for NO biosynthesis.
59x44mm (300 x 300 DPI)
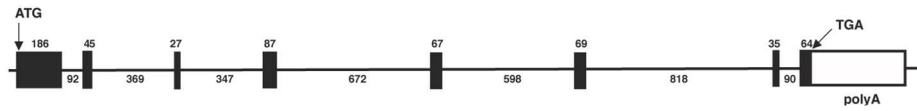
```
MAIARTHMFGVVNFQLNEAPMAFAGSSAILWHHGERSQRNVALRRRGNAM
IVPRIRAQSSASEYVPDSKFYKVEAILRPWRVPLVSSALLNMGIRGVTVS
DVRGFGAQGGSKERQGGSEFSEDNFVAKVKMEIVVRNDQVEAVIDKIIEE
ARTGEIGDGKIFLIPVSDVIRVRTGERGEQAERMTGGRTDILSTV
```

Intron/exon organization of the LjGLB1 gene. Numbers above exons (black boxes) and below introns (lines) indicate their length in nucleotides. The positions of the start (ATG) and stop (TGA) codons are indicated. The amino acid sequence of the L. japonicus PII protein is shown at the bottom.
132x42mm (300 x 300 DPI)
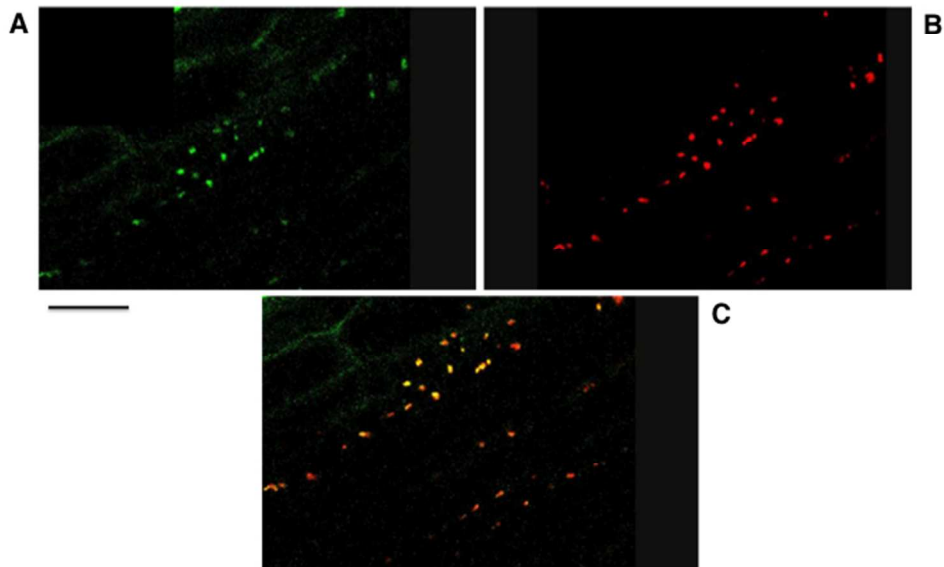
Subcellular localization of the PII protein. Confocal laser scanning micrographs of L. japonicus hairy roots stably expressing the 35S-LjGLB1-GFP (A) and AtrecA-DsRed2 (B) fusions. In the merged image (C) the co-localized signals of green GFP and red DsRed2 fluorescence appears yellow. Bar = 50 µm.
254x190mm (72 x 72 DPI)
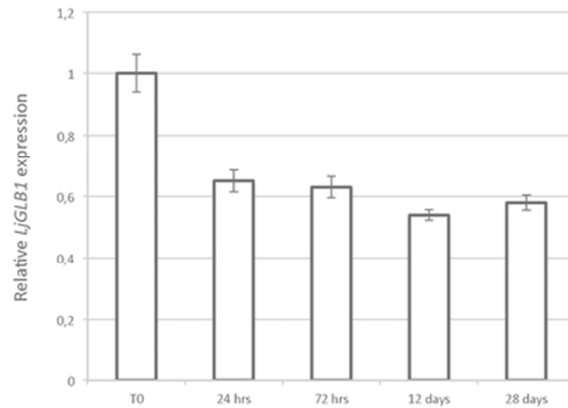
Time course of the LjGLB1 transcriptional regulation in root and nodules tissues after M. loti inoculation.
RNAs were extracted from roots of seedlings grown in presence of $10\mu M$ NH4NO3 (T0) and at different times
after inoculation (24 hrs, 72 hrs) and from young (12 days) and mature nodules (28 days). Expression
levels were normalized with respect to the internal control ubiquitin (UBI) gene and plotted relative to the
expression of T0. Data bars represent the mean and standard deviations of data obtained with RNA
extracted from three different sets of plants and 3 real-time PCR experiments.
59x44mm (300 x 300 DPI)
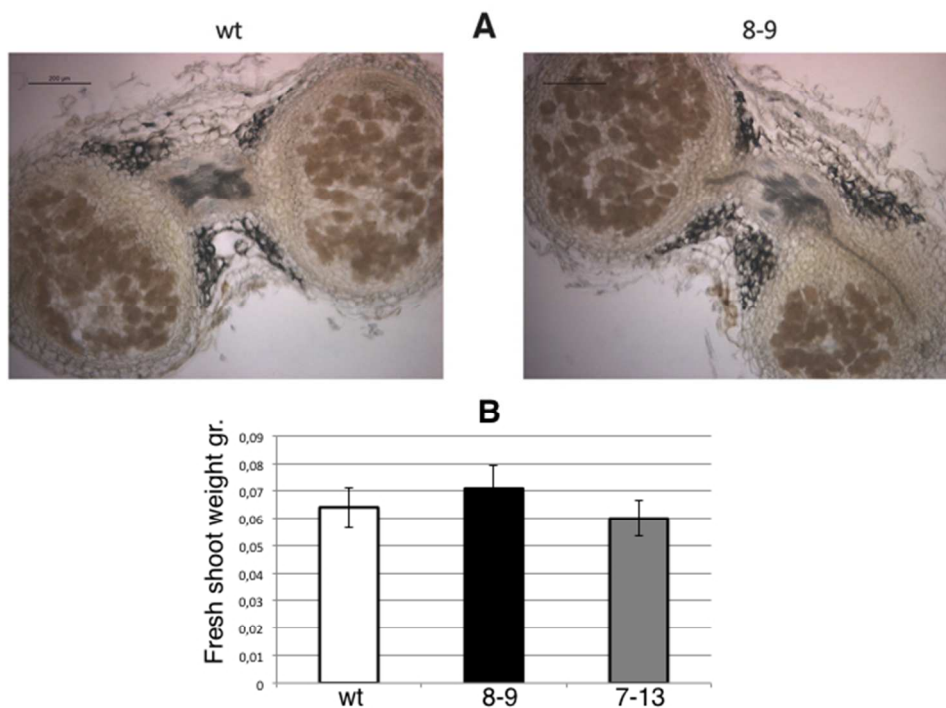
A, 60 μm thick sections of representative four weeks old nodules of wild type and 8-9 plants. No differences are observed in nodule diameter and density of invaded cells. B, Fresh shoot weigth of wild type, 7.13 and 8-9 plants four weeks after inoculation. Plants were germinated on H2O agar, and 7 days old seedlings transferred on Gamborg B5 derived medium with 10 μM NH4KNO3 as sole N source and inoculated with M. loti. Data represent the mean and standard error obtained from three independent experiments (15 plants per experiment).
254x190mm (72 x 72 DPI)